Resource

Cell Reports

SUMO Signaling by Hypoxic Inactivation of SUMO-Specific Isopeptidases

Graphical Abstract

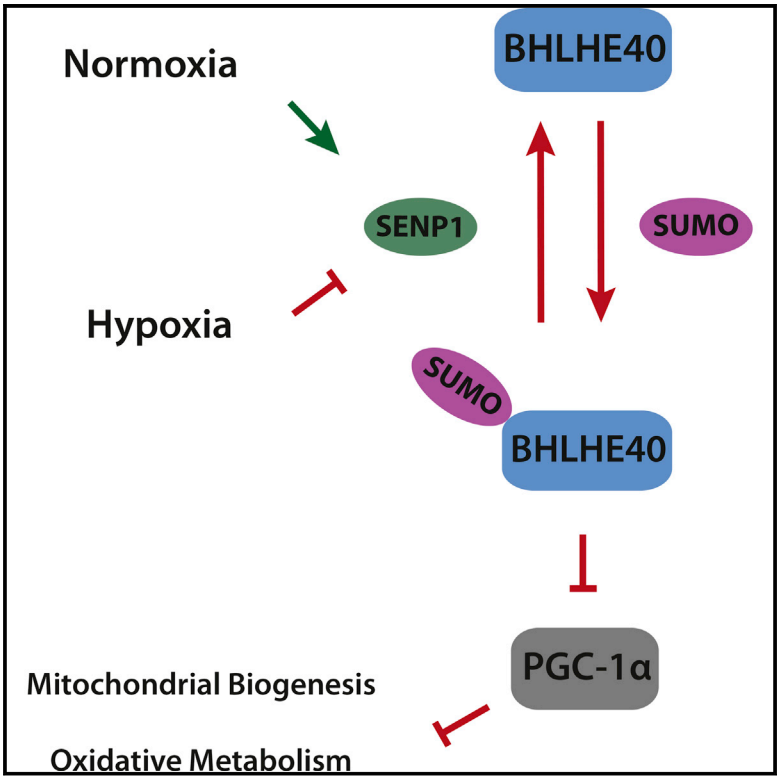

Highlights

- The activity of distinct SUMO isopeptidases is impaired under hypoxia
- SUMO modification of a subset of target proteins is altered in hypoxia
- Transcriptional regulator BHLHE40 is a hypoxic SUMO target
- SUMOylation of BHLHE40 may contribute to metabolic reprogramming under hypoxia

Authors

Kathrin Kunz, Kristina Wagner, Luca Mendler, Soraya Hölper, Nathalie Dehne, Stefan Müller

Correspondence

ste.mueller@em.uni-frankfurt.de

In Brief

Kunz et al. find that SUMO signaling in hypoxia is altered by inactivation of SUMO-specific isopeptidases. Using proteomic analysis, they define a subset of hypoxia-induced SUMO1 targets and propose that hypoxia-induced SUMOylation of the transcriptional co-repressor BHLHE40 contributes to metabolic reprogramming under these conditions.

Kunz et al., 2016, Cell Reports *16*, 3075–3086
September 13, 2016
http://dx.doi.org/10.1016/j.celrep.2016.08.031

CellPress

Cell Reports
Resource

SUMO Signaling by Hypoxic Inactivation of SUMO-Specific Isopeptidases

Kathrin Kunz,[1,3] Kristina Wagner,[1,3] Luca Mendler,[1] Soraya Hölper,[1] Nathalie Dehne,[2] and Stefan Müller[1,4,*]
[1]Institute of Biochemistry II, Goethe University, Medical School, Theodor-Stern-Kai 7, 60590 Frankfurt, Germany
[2]Institute of Biochemistry I, Goethe University, Medical School, Theodor-Stern-Kai 7, 60590 Frankfurt, Germany
[3]Co-first author
[4]Lead Contact
*Correspondence: ste.mueller@em.uni-frankfurt.de
http://dx.doi.org/10.1016/j.celrep.2016.08.031

SUMMARY

Post-translational modification of proteins with ubiquitin-like SUMO modifiers is a tightly regulated and highly dynamic process. The SENP family of SUMO-specific isopeptidases comprises six cysteine proteases. They are instrumental in counterbalancing SUMO conjugation, but their regulation is not well understood. We demonstrate that in hypoxic cell extracts, the catalytic activity of SENP family members, in particular SENP1 and SENP3, is inhibited in a rapid and fully reversible process. Comparative mass spectrometry from normoxic and hypoxic cells defines a subset of hypoxia-induced SUMO1 targets, including SUMO ligases RanBP2 and PIAS2, glucose transporter 1, and transcriptional regulators. Among the most strongly induced targets, we identified the transcriptional co-repressor BHLHE40, which controls hypoxic gene expression programs. We provide evidence that SUMOylation of BHLHE40 is reversed by SENP1 and contributes to transcriptional repression of the metabolic master regulator gene PGC-1α. We propose a pathway that connects oxygen-controlled SENP activity to hypoxic reprogramming of metabolism.

INTRODUCTION

Members of the ubiquitin-like SUMO system function as post-translational modifiers in all eukaryotes (Flotho and Melchior, 2013; Gareau and Lima, 2010; Wilkinson and Henley, 2010). In human cells, three SUMO forms (SUMO1, SUMO2, and SUMO3) can be covalently attached to lysine residues of target proteins. Because SUMO2 and SUMO3 are highly related to each other, they are generally treated as a single entity and referred to as SUMO2/3. All SUMO forms are synthesized as precursor proteins that require proteolytic processing at their C terminus to enter the conjugation pathway. In humans, this cleavage is catalyzed by cysteine proteases, termed SUMO-specific isopeptidases, SUMO hydrolases, or SUMO proteases of the Ulp/SENP (ubiquitin-like protease/sentrin-specific protease) family or USPL1 (ubiquitin-specific peptidase-like protein 1) (Hickey et al., 2012; Huang et al., 2015; Mukhopadhyay and Dasso, 2007; Nayak et al., 2014; Yeh, 2009). These enzymes clip off the terminal residues of SUMO that follow a C-terminal diGlycine motif, whose accessibility is indispensable for the subsequent activation and conjugation of SUMO. After processing, SUMO is activated in an ATP-dependent process by the dimeric (AOS1/UBA2) E1 activating enzyme and subsequently transferred to the E2 conjugating enzyme Ubc9. Attachment to target proteins is finally done by Ubc9 alone or with the help of E3 SUMO ligases, such as RanBP2 or members of the PIAS family (Flotho and Melchior, 2013; Gareau and Lima, 2010; Wilkinson and Henley, 2010). A typical consequence of SUMO conjugation is the alteration of protein-protein interactions (Jentsch and Psakhye, 2013; Raman et al., 2013). The fate of a SUMO-protein conjugate is often related to the recognition of an interaction partner that harbors a distinct SUMO interaction module (SIM). Regulated deconjugation of SUMO from target proteins is a central element of the SUMO pathway, because deconjugation guarantees the plasticity of protein interaction networks. The known mammalian SUMO-specific isopeptidases or proteases belong to three distinct families: Ulp/SENP, Desi (deSUMOylating isopeptidase), and USPL1 (Hickey et al., 2012; Huang et al., 2015; Mukhopadhyay and Dasso, 2007; Nayak et al., 2014; Yeh, 2009). The Ulp/SENP family, which is the best-characterized group, consists of six members. Within their catalytic domains, SENPs share 20% to 60% sequence identity. The SENP1/SENP2, SENP3/SENP5, and SENP6/SENP7 pairs exhibit the highest degree of similarity to each other. Distinct family members function as deconjugating enzymes for isopeptide-linked SUMO-protein conjugates or depolymerize isopeptide-linked poly-SUMO2/3 chains (Nayak and Müller, 2014). Moreover, some family members act as processing enzymes for the C-terminal maturation of the SUMO precursor.

Because of detailed structural and biochemical work, we gained a thorough mechanistic understanding of SENP function (Lima and Reverter, 2008; Reverter and Lima, 2004, 2006; Shen et al., 2006a, 2006b; Xu et al., 2006). Structural data of the catalytic domain uncovered the catalytic mechanism of this enzyme class. The active site cysteine residue is embedded in a typical catalytic triad (cysteine-histidine-aspartic acid [Cys-His-Asp]) with a conserved glutamine (Gln) residue in proximity stabilizing

the transition state during catalysis. The substrate enters the catalytic site through a tunnel, in which conserved tryptophan (Trp) residues position the diglycine motif and the scissile bond over the active site.

Despite these detailed mechanistic insights, the physiological role of distinct SENP family members and their regulation is only partially understood. In this work, we show that the cellular oxygen supply is a critical determinant for the activity of distinct SENP family members. Hypoxia defines a situation in which the oxygen supply is below the physiological requirements. Hypoxia occurs in various pathophysiological conditions, such as ischemia or reperfusion injury or cancer (Semenza, 2014). A typical consequence of hypoxia is a reduced capacity to produce energy through oxidative phosphorylation. To cope with this problem, cells activate an adaptation mechanism, which is primarily triggered by the hypoxia-induced transcription factor HIF1α (Kenneth and Rocha, 2008). In normoxia HIF1α is constantly degraded by the ubiquitin-proteasome system, but rapidly stabilized under hypoxic conditions. This fosters the induction of HIF1α target genes, which typically promote angiogenesis and anaerobic ATP production through glycolysis.

Here we provide evidence that the ubiquitin-like SUMO system contributes to the hypoxic response. In particular, we show that the activity of the SUMO deconjugases SENP1 and SENP3 is highly sensitive to oxygen deprivation. We propose that this enhances SUMOylation of a subset of cellular proteins and contributes to the adaptation of cellular metabolism to hypoxic conditions.

RESULTS

Hypoxia-Induced SUMOylation Is Accompanied by Reduced Activity of SUMO Hydrolases

Protein modification by SUMO paralogs is a highly dynamic process. However, the signals that control the balance of SUMO conjugation and deconjugation are not well defined. Low oxygen was reported to enhance SUMO modification, but the underlying mechanism has remained unclear (Agbor et al., 2011). In addition, most studies on hypoxia-mediated control of SUMOylation were performed in cells that stably or transiently overexpress SUMO paralogs. To monitor whether conjugation by endogenous SUMO forms is altered in response to limited oxygen supply, we incubated HeLa cells under normoxic conditions or at 1% oxygen for 1, 2, 4, or 24 hr. At each time point, cell extracts were prepared under denaturing conditions and the state of SUMO conjugation was detected by anti-SUMO1 or anti-SUMO2/3 immunoblotting (Figure 1A). To control for the cellular response to hypoxia, HIF1α levels were followed by anti-HIF1α immunoblotting. As expected, hypoxia triggers strong and rapid stabilization of HIF1α that is visible in the anti-HIF1α immunoblot. SUMO conjugates are also drastically enhanced in hypoxia. In normoxic control cells, the typical 90 kDa RanGAP1-SUMO1 conjugate can be detected in anti-SUMO1 immunoblots. In cells kept under hypoxic conditions for 24 hr, high-molecular SUMO1 conjugates migrating above the 90 kDa RanGAP1-SUMO1 conjugate become detectable. This conjugation pattern is characteristic for enhanced SUMO modification in different cellular stress situations. At longer exposure, the accumulation of these conjugates is visible at earlier time points. Similar to what was observed for SUMO1, SUMO2 conjugates, particularly high-molecular-weight forms, are increased in response to hypoxia, albeit to a lower extent. Altogether, these data support the idea that hypoxia induces SUMOylation of cellular proteins and in particular triggers the formation of high-molecular-weight conjugates.

One possible explanation of hypoxia-stimulated SUMOylation could be the induction of SUMO paralogs. However, proteome analysis by mass spectrometry (MS) or mRNA analysis by qRT-PCR did not reveal a significant increase in expression of SUMO1, SUMO2, or SUMO3 (Figures S1A and S1B). Moreover, levels of Ubc9 or PIAS family members remained unaltered under hypoxia. We therefore hypothesized that alteration in SUMO deconjugation may account for increased SUMOylation in hypoxia. To follow this idea, we measured the cellular activity of SUMO hydrolyzing enzymes in normoxic and hypoxic cells by using a fluorescence-based activity assay. SUMO1- and SUMO2-amidomethylcoumarine (SUMO1-AMC and SUMO2-AMC) are sensitive fluorogenic substrates for SUMO hydrolases, including SENP enzymes. In these reagents, AMC is linked to the C terminus of SUMO1 or SUMO2 through an amide bond, which is specifically hydrolyzed by SENPs (Kolli et al., 2010; Wilkinson et al., 2005). AMC is quenched when coupled to SUMO, but upon release it can be measured by emitted fluorescence (Madu and Chen, 2012). SUMO1 or SUMO2-AMC probes therefore allow the monitoring of SENP activity in cell extracts by following the increase in fluorescence over time. To determine oxygen-controlled SUMO protease activity, cell extracts were prepared from normoxic cells or from cells kept under hypoxia for different time points and incubated with SUMO1-AMC or SUMO2-AMC. Data from a representative experiment are shown in Figures 1B and 1C. Generally, normoxic control cells exhibit high cleavage activity toward SUMO2-AMC and lower activity toward SUMO1-AMC. However, in cells kept under hypoxia, the activity toward both SUMO1-AMC and SUMO2-AMC was greatly reduced. For SUMO1-AMC and SUMO2-AMC, cleavage activity was consistently reduced to 40%–50% already after 2–4 hr. After 24 hr, this was even more drastic, with SUMO1 cleavage activity reduced to 30% and SUMO2 cleavage activity reduced to less than 20%. A reoxygenation period of 30 min was sufficient for the full recovery of SENP activity following 4 or 24 hr of hypoxia. Altogether, these findings support the idea that the induction of SUMO conjugation by oxygen deprivation is linked to reversible downregulation of SUMO protease activity.

Hypoxia Inhibits the Catalytic Activity of SENP1 and SENP3

It has been reported that levels of SENP family members are regulated by changes in gene expression or protein turnover (Cimarosti et al., 2012; Guo et al., 2013; Huang et al., 2009; Kuo et al., 2008; Yan et al., 2010). Therefore, we tested whether the reduction of SUMO hydrolyzing activity could be linked to altered steady-state levels of SENP family members. Immunoblots again revealed an increase in HIF1α, as well as SUMO conjugation under hypoxia, but we did not detect a significant change in the amount of SENP1, SENP2, SENP3, SENP5, and SENP7 in cells kept under hypoxic conditions for different time

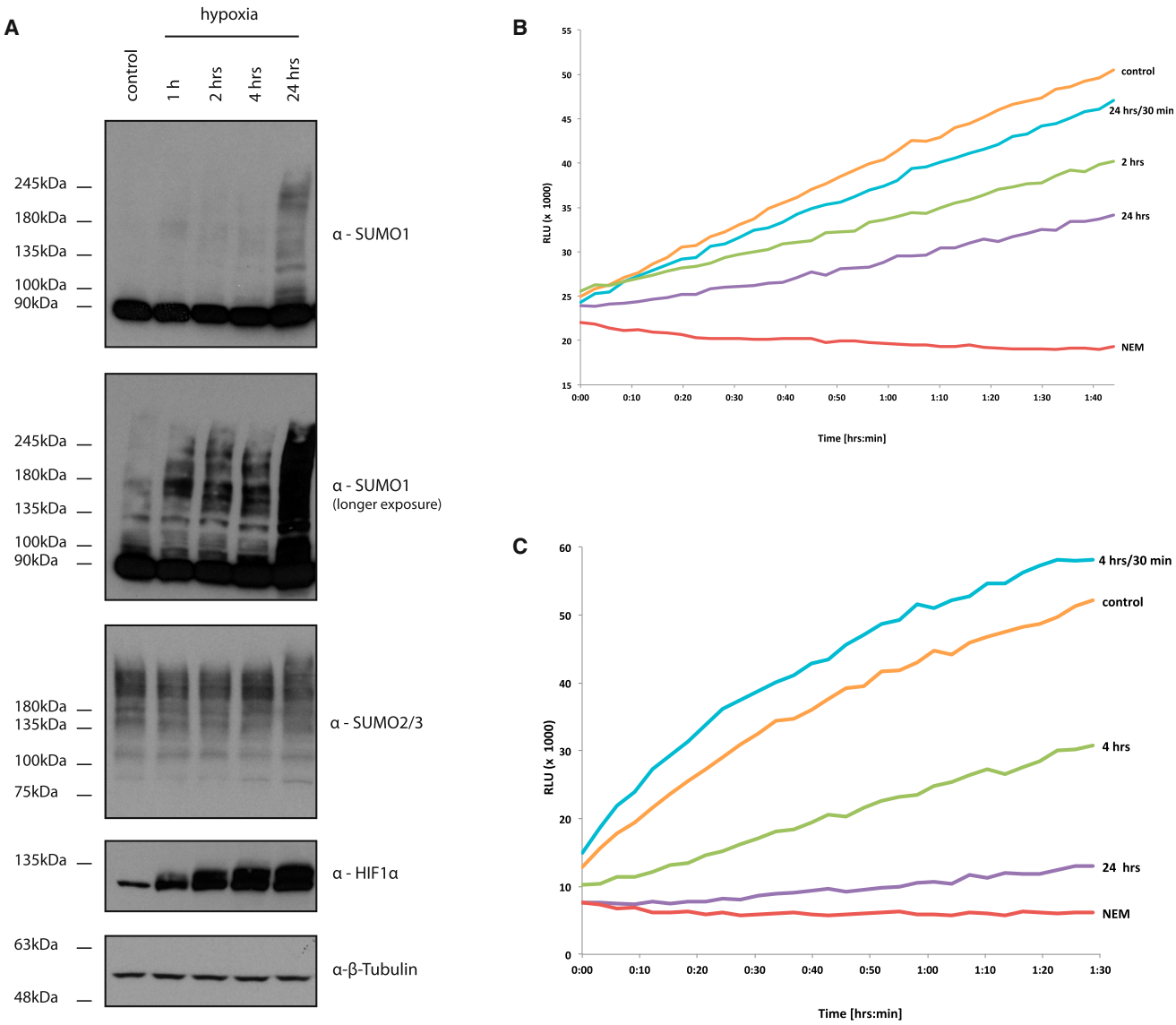

Figure 1. Hypoxia-Induced SUMOylation Is Accompanied by Reduced Activity of SUMO Hydrolases

(A) HeLa cells were cultured under normoxic conditions (5% CO_2) or hypoxic conditions (1% O_2) for indicated times, cells were lysed in SDS-PAGE buffer, and proteins were separated by SDS-PAGE. After western transfer, immunoblotting was performed using anti-SUMO1, anti-SUMO2/3, anti-HIF1α, or anti-β-Tubulin antibody. Tubulin served as a loading control.

(B) SUMO protease activity in cell extracts from normoxic, hypoxic, or hypoxic and reoxygenated HeLa cells was determined by measuring fluorescence signals (relative light unit [RLU]) emitted from liberated AMC substrate (SUMO1-AMC) over time. As negative control, cells were treated with NEM (10 mM) to inhibit cysteine protease activity of SUMO proteases.

(C) As in (B), using SUMO2-AMC as the substrate.

points (Figure S2A). Only in the case of SENP6 did we observe a reduced protein level after prolonged incubation under hypoxic conditions. Altogether, this indicates that the reduced SUMO1 or SUMO2 hydrolyzing activity in hypoxic cell extracts is not primarily due to reduced protein levels of SENP family members.

Based on this observation, we reasoned that hypoxia might directly affect the catalytic activity of SENPs. To address this point, we used hemagglutinin (HA)-tagged SUMO-vinylsulfone (VS) derivatives, which function as active site-directed probes for SENPs through irreversible covalent modification of their catalytic cysteine residue (Madu and Chen, 2012). When added to a cell extract, active SENPs are labeled by HA-SUMO-VS and can be detected by anti-HA antibody (Madu and Chen, 2012). Accordingly, upon addition of HA-SUMO1-VS or HA-SUMO2-VS to cell extracts, distinct bands at 180, 95, and 75 kDa are detected (Figure S2B). Upon addition of N-ethylmaleimide (NEM), which inactivates cysteine proteases through alkylation of their catalytic residues, all HA-reactive bands disappear. This indicates that these adducts represent noncleavable thioether bonds of SUMO with the catalytic cysteine residues. The signal

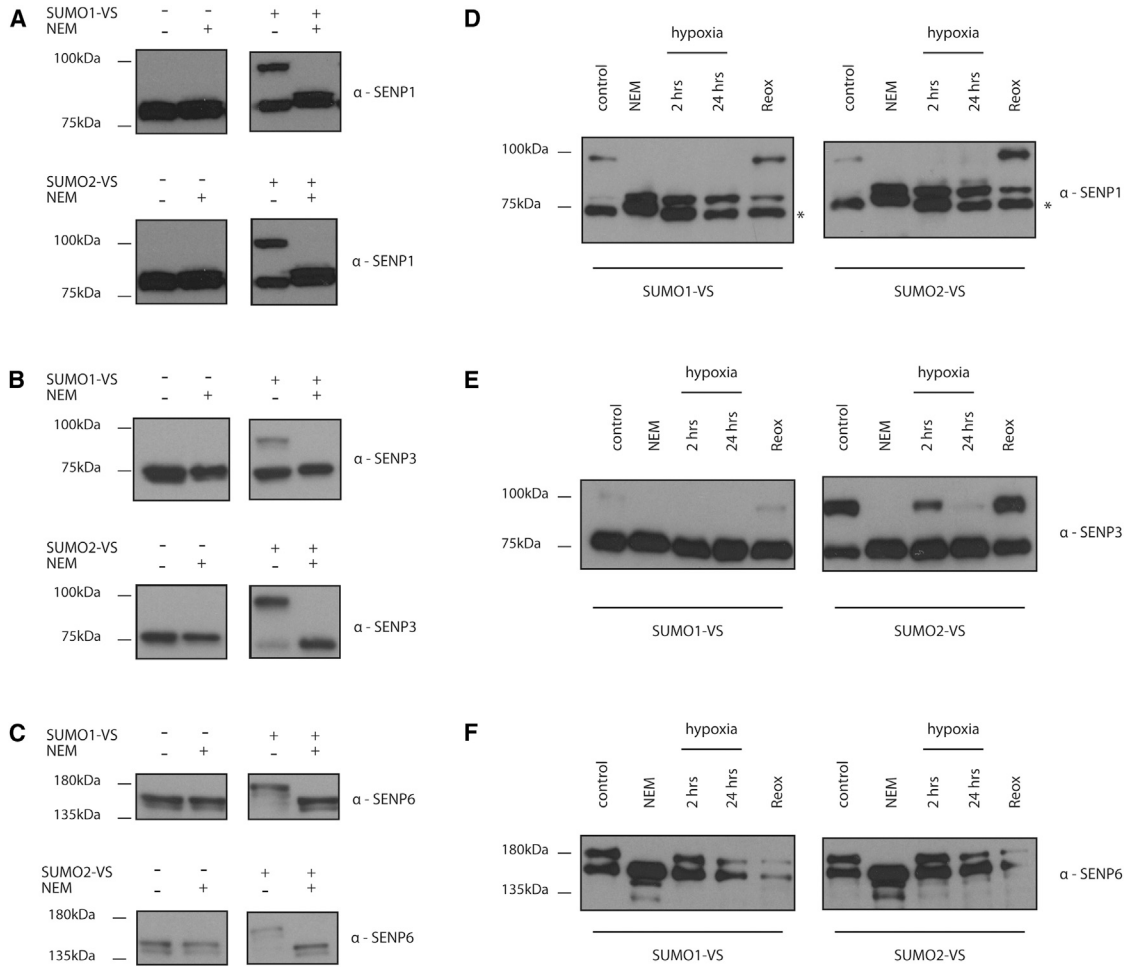

Figure 2. SENP1 and SENP3 Activity Is Sensitive to Hypoxia

(A) Total HeLa cell extracts prepared in SEM buffer were incubated with or without HA-SUMO1-VS or HA-SUMO2-VS as indicated for 15 min at 25°C. After separation by SDS-PAGE, immunoblots were probed with anti-SENP1 antibody. NEM was added as a negative control where indicated.

(B) As in (A), but anti-SENP3 antibody was used for detection.

(C) As in (A), but anti-SENP6 antibody was used for detection.

(D–F) HeLa cells were cultured under normoxia, hypoxia, or hypoxia and reoxygenation (24 hr hypoxia/30 min reoxygenation) as indicated. Lysates were prepared as in (A)–(C), and samples were incubated with either HA-SUMO1-VS or HA-SUMO2-VS for 15 min at 25°C and blotted against SENP1 (D), SENP3 (E), or SENP6 (F). Where indicated, NEM was added to the sample as a negative control. In (D), the asterisk marks an unspecific band detected by anti-SENP1 antibody. All blots in individual sections were run on the same gel.

for the prominent SUMO1-VS or SUMO2-VS adducts migrating at 95 kDa were drastically reduced after 2 hr of hypoxia and further diminished after 24 hr, indicating a drop of catalytic activity (Figure S2C). A 30 min period of reoxygenation after 24 hr of hypoxia triggered the full recovery of activity, as demonstrated by the reappearance of the 95 kDa SUMO1-VS or SUMO2-VS adducts. In contrast to the 95 kDa signal, the 180 kDa signal did not vanish but was reduced under hypoxia (Figure S2C). Altogether, these data support the idea that hypoxia affects the enzymatic activity of SUMO-specific isopeptidases.

To further investigate whether distinct SENP family members are controlled by hypoxia, we first measured the activity of specific SENPs in HeLa cell extracts. To this end, extracts from HeLa cells, which had been incubated with SUMO1-VS or SUMO2-VS, were probed with antibodies directed against distinct SENPs (Figures 2A–2C; Figure S3). For SENP2, SENP5, and SENP7, we could not detect specific SUMO1-VS or SUMO2-VS adducts due to either the lack of specific antibodies or their low activity in HeLa cells (Figure S3). In the case of SENP1, however, a 95 kDa SUMO1-VS or SUMO2-VS form was readily detectable upon addition of SUMO1-VS or SUMO2-VS to cell extracts (Figure 2A). SENP1 is equally well converted to the SUMO1-VS or SUMO2-VS form, which is consistent with the idea that it exerts cleavage activity toward both SUMO1 and SUMO2 conjugates. In both cases, addition of NEM abrogated SUMO-VS adduct formation, demonstrating specificity of the reaction. Similar to what observed for SENP1, anti-SENP3-reactive NEM-sensitive SUMO1-VS or SUMO2-VS adducts migrating at 95 kDa were detected (Figure 2B). SENP3 is more active toward SUMO2 conjugates, but at least in our experimental setting, a fraction can be

converted to a SUMO1-VS conjugate. In the case of SENP6, NEM-sensitive anti-SENP6-reactive SUMO1-VS or SUMO2-VS adducts migrating at 180 kDa were detected (Figure 2C). Altogether, these data indicate that the 95 kDa anti-HA-reactive SUMO1-VS or SUMO2-VS conjugates visible in Figure S2B correspond to SENP1 and SENP3, while the 180 kDa conjugate is a SUMO1 or SUMO2-SENP6 form.

We next monitored the activity of SENP1, SENP3, and SENP6 in cells cultured for 2 or 24 hr in low oxygen (Figures 2D–2F). Under these conditions, no SENP1-SUMO1-VS or SENP1-SUMO2-VS adducts were formed, demonstrating almost complete loss of enzymatic activity (Figure 2D). However, in extracts from cells that had undergone 30 min of reoxygenation after 24 hr of hypoxia, SENP1 activity toward both SUMO1 and SUMO2 was fully restored. A similar scenario was observed for SENP3 activity (Figure 2E). In normoxic cells, a fraction of SUMO1-VS is converted to a SENP3 conjugate, which is consistent with its limited activity toward SUMO1. In hypoxic cells, however, no SUMO1-VS adducts were detectable, while a 30 min reoxygenation period was sufficient to restore activity. The activity of SENP3 toward SUMO2 was also significantly reduced in cells kept for 2 hr in hypoxia and was almost undetectable after 24 hr. Reoxygenation again fully restored activity. Altogether, these results indicate that the activity of SENP1 and SENP3 is highly sensitive to changes in oxygen concentration. In hypoxia, the activity of both enzymes is inhibited in a rapid and fully reversible process. When monitoring SENP6 activity, we did not observe any reduction in activity toward SUMO1 or SUMO2 in cells kept for 2 hr under hypoxia (Figure 2F). At later time points (24 hr of hypoxia), we noticed a general reduction of SENP6 levels, a phenomenon that was even more pronounced upon reoxygenation. However, SENP6 was still enzymatically active after 24 hr of hypoxia. Altogether, this demonstrates that both SENP1 and SENP3, but not SENP6, activity is highly sensitive to alterations in cellular oxygen levels.

Hypoxia Alters SUMO Conjugation of a Distinct Subset of Cellular Proteins

Given that SENP1 is active toward SUMO1 and SUMO2 while SENP3 preferentially acts on SUMO2 conjugates, we reasoned that it is primarily the inactivation of SENP1 that triggers the accumulation of SUMO1 conjugates in hypoxic cells. In line with this idea, the SUMO1 conjugation pattern induced in hypoxic cells resembles the accumulation of SUMO1 conjugates upon small interfering RNA (siRNA)-mediated depletion of SENP1 (Figure 3A). SENP3 depletion only minimally induced SUMO1 conjugation, and the combination of SENP3 siRNA and SENP1 siRNA only moderately increased SUMO1 conjugates when compared to depletion of SENP1 alone.

To more specifically identify the subset of cellular regulators that exhibit enhanced conjugation to SUMO1 in hypoxia, we followed a MS-based proteomic approach. HeLa cells were cultured under normoxic conditions or under hypoxia for 24 hr, and endogenous SUMO1 conjugates were immunopurified under denaturing conditions according to an established procedure (Becker et al., 2013). Immunopurified material was released from beads by SUMO1 peptide elution, separated by SDS-PAGE, and digested by trypsin, and peptides were measured by liquid chromatography-tandem mass spectrometry (LC-MS/MS), followed by relative label-free quantification using the Max label-free quantification (LFQ) algorithm (Cox et al., 2014). To assure accurate quantification of SUMO1 conjugates in normoxic and hypoxic conditions, the experiment was performed in triplicate, and control immunoprecipitation (IP) using mouse immunoglobulin G (IgG) was done for each condition. Pearson correlation coefficient determination revealed almost linear correlation ($r > 0.9$) of LFQ intensities for the SUMO1 IP experiments in normoxic and hypoxic cells. Moreover, principal-component analysis showed high similarity among the triplicates (Figure S4A). The entire dataset is given in Table S1.

In normoxia, we identified 143 SUMO1 targets that were enriched more than 4-fold in anti-SUMO1 immunoprecipitates when compared to IgG controls (Figure 3B; Figure S4B). The data show a good overlap to SUMO targets identified by Becker et al. (2013). In hypoxic cells, we defined a set of 135 proteins as specific SUMO1 conjugates (Figure 3C; Figure S4C). Among these, 83 were common to normoxia (Figure 3B). Most hypoxic SUMO substrates did not show a significant change in modification when compared to normoxia. However, 48 proteins were at least 2-fold more enriched in SUMO1 IPs from hypoxic cells when compared to normoxic cells (Figure 3C). Among these, 30 exhibited at least 3-fold stronger enrichment (Figure 3C). The E3 SUMO ligases RanBP2 and PIAS2 are found within the group of most highly regulated proteins (>8-fold stronger SUMOylation in hypoxia). Both RanBP2 and PIAS2 undergo autoSUMOylation, which under normal conditions is likely limited by SENPs. Another large subgroup of strongly enriched SUMO targets in hypoxia (>5-fold stronger SUMOylation in hypoxia) is composed of transcriptional repressors, such as FSBP, NAB1, BHLHE40, KCTD1, KCTD15, or ETV6 (Figure 3C). Transcriptional and chromatin regulators (GTF2IRD1, IRF2BP1, CTCF, BCLAF1, ATRX, Wiz, NAP1L, or SUPT16H) are also enriched within the group of moderately regulated hypoxia-induced SUMO1 targets (2- to 3-fold induced in hypoxia) (Figure 3C). As discussed in detail later, some were already reported to play a role in HIF1α signaling, raising the possibility that the SUMO system contributes to the alterations of gene expression programs in hypoxia. The increased hypoxic SUMOylation of the candidates mentioned earlier is not primarily due to alteration in protein levels, as monitored by proteomic data in normoxic and hypoxic cell lysates (Table S1). This is different from the proteasomal subunits PSMA6 and PSMB4/5/6, in which enhanced SUMOylation in hypoxia correlates with elevated protein amounts in cell extracts (Table S1). Whether this is due to induction of gene expression or SUMO-dependent changes in protein stability remains to be determined. According to our dataset, 30 proteins exhibit at least 4-fold reduced SUMO1 conjugation in hypoxia when compared to normoxia (Table S1). For a subset of these candidates (13 of 30), reduced SUMOylation correlates with an at least 2-fold reduced protein amount in hypoxic cell extracts. These candidates include RSF1 and BRD8, which were among the most strongly downregulated SUMO1 targets in our dataset. As discussed in detail later, both proteins were also defined as putative downregulated SUMO3 targets in a cellular model of ischemia (Yang et al., 2012).

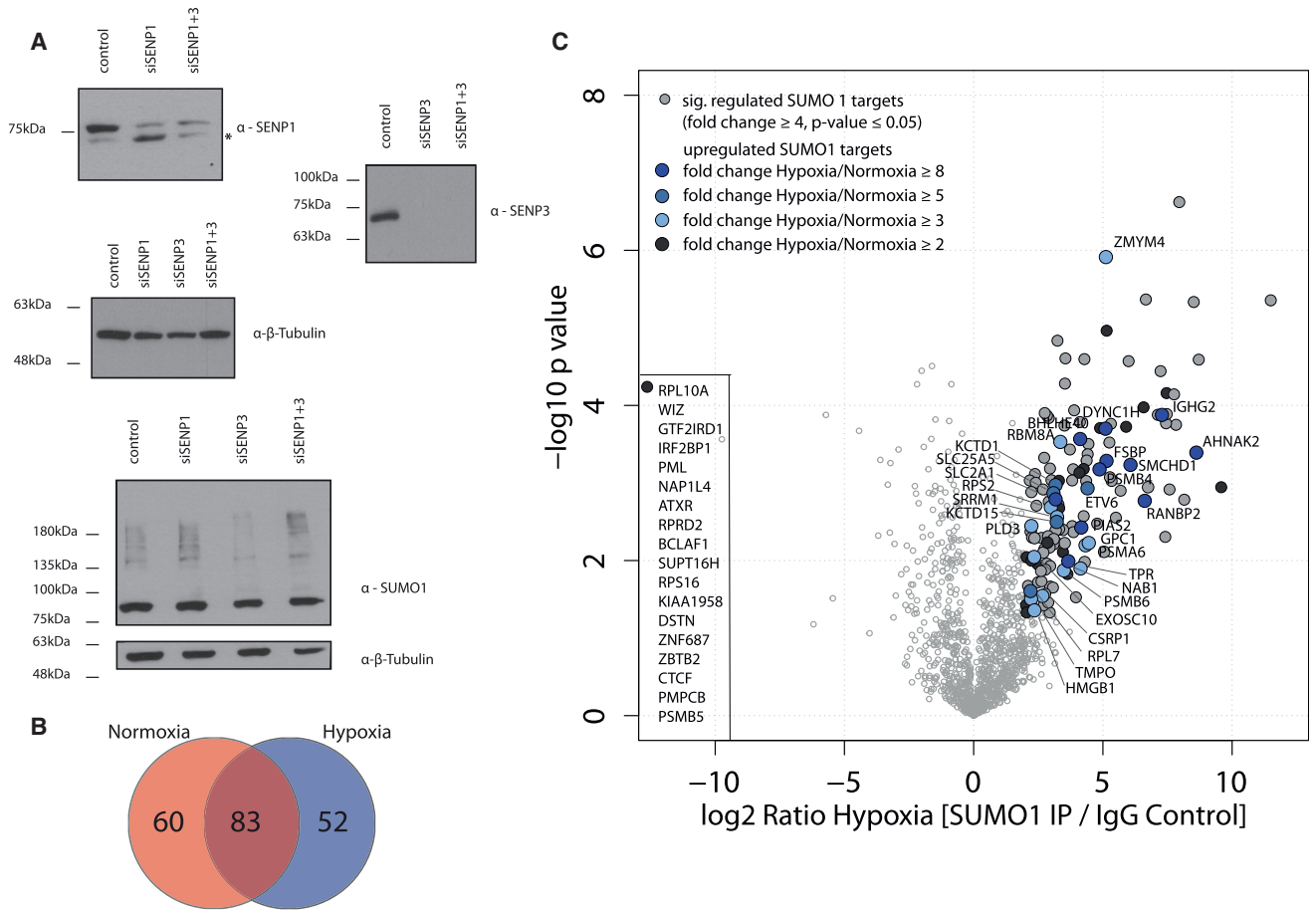

Figure 3. Hypoxia Triggers SUMO Conjugation to a Distinct Subset of Cellular Proteins

(A) HeLa cells were transfected with control siRNA or siRNA directed against SENP1, SENP3, or both, and cell lysates were prepared in SDS-PAGE sample buffer. Knockdown of the respective target gene was validated by immunoblotting against SENP1 or SENP3 (upper panels). The effect of siRNA-mediated knockdown of SENP1, SENP3, or SENP1/3 on SUMO1 conjugates was monitored by immunoblotting with anti-SUMO1 antibody (lower panel).

(B) Venn diagram indicating an overlap of 83 SUMO1-target proteins quantified in each condition. In normoxia and hypoxia, 143 and 135 proteins, respectively, were significantly enriched upon immunopurification on anti-SUMO1 beads. Proteins with a 4-fold enrichment over IgG control and a p value < 0.05 are considered high-confidence SUMO1 targets.

(C) Volcano blot summarizing the results from quantitative MS on SUMO1 conjugates immunopurified from hypoxic cells kept for 24 hr in hypoxia. For the identification of high-confidence SUMO1 targets, a Student's t test comparing the LFQ intensities of the anti-SUMO1 IP and the LFQ intensity of the IgG control was used. SUMO1 targets were visualized by plotting the difference of the log2 mean protein intensities between the SUMO1 IP and the IgG control against the negative logarithmized p values. Proteins with 4-fold enrichment over the IgG control and a p value < 0.05 are considered high-confidence SUMO1 targets (designated as significantly regulated). All SUMO1 targets that were at least 2-fold more enriched in SUMO1 IPs from hypoxic cells compared to normoxic cells are colored as indicated. Proteins with a negative log2 intensity (SUMO1 IP/IgG) in normoxic cells were excluded from the analysis.

Altogether, these data indicate that hypoxia alters SUMO conjugation of a distinct subset of cellular proteins.

BHLHE40 Is a SENP-1-Regulated Hypoxic SUMO Target Possibly Involved in Metabolic Reprogramming under Hypoxia

Among the most strongly regulated hypoxic SUMO targets, we identified the transcriptional co-repressor BHLHE40. Because BHLHE40 is known to be involved in cellular adaptation to a hypoxic environment, we further investigated this pathway (Kato et al., 2014). First, we set out to validate the MS data by immunoblotting (Figure 4A). SUMO1 conjugates were immunopurified from normoxic or hypoxic cell lysates under denaturing conditions, and SDS-PAGE immunoblotting was performed with anti-BHLHE40 antibody. In both normoxic and hypoxic cell extracts, BHLHE40 can be detected around 55 kDa. However, a SUMO1-BHLHE40 conjugate migrating at 70 kDa was only recovered from hypoxic, not normoxic, cells (Figure 4A). In accordance with MS data and published work, the amount of BHLHE40 was higher under hypoxia. However, even after longer exposure, no SUMOylated form of BHLHE40 was detectable in normoxic cell lysates, indicating that the modification is specifically induced in hypoxia (Figure S5). To further support these data, HeLa cells that express a single copy of His-tagged SUMO1 under the control of a tetracycline-inducible promoter were incubated under normoxia or hypoxia

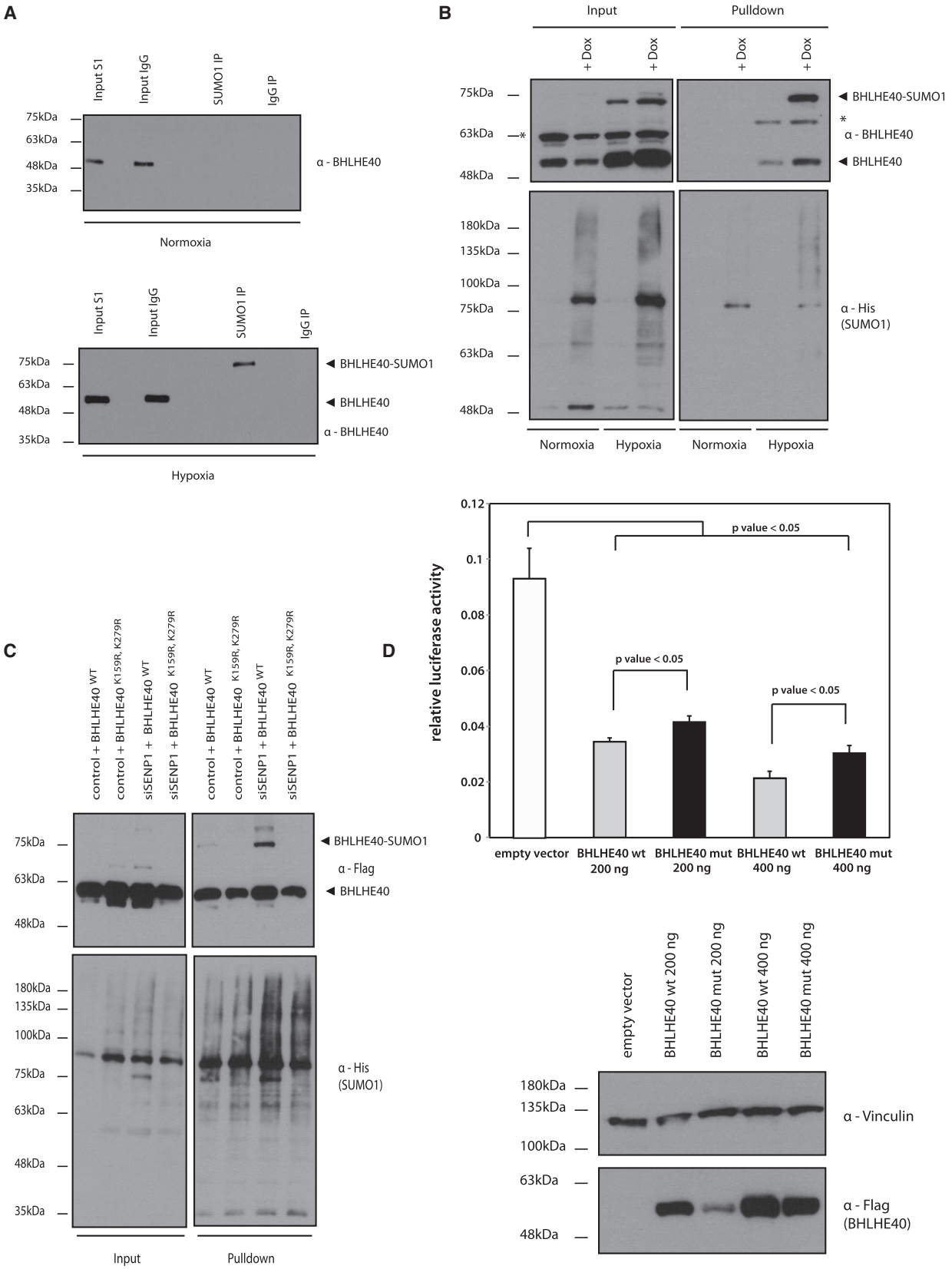

(legend on next page)

(Ullmann et al., 2012). After cell lysis, His-SUMO1 conjugates were captured on nickel-nitrilotriacetic acid (Ni-NTA) beads. Following SDS-PAGE, BHLHE40 and His-SUMO1 expression was detected by anti-BHLHE40 immunoblotting (Figure 4B). In the input samples, BHLHE40 levels were again elevated in hypoxic cell extracts when compared to control. Only in hypoxic samples was a prominent 70 kDa anti-BHLHE40-reactive form detectable in addition to the major 55 kDa species. The amount of this 70 kDa form was higher upon induction of His-SUMO1 expression, suggesting that it corresponds to a BHLHE40-SUMO1 conjugate that under hypoxia is formed by endogenous SUMO1 but can be further induced when His-SUMO1 is expressed. In agreement with this assumption, the 70 kDa species was specifically enriched on Ni-NTA beads under hypoxic conditions and when His-SUMO1 expression was induced (Figure 4B). Altogether, these data demonstrate that inhibition of SENP1 activity in oxygen-deprived cells can trigger SUMO1 conjugation to BHLHE40. To provide direct evidence that BHLHE40 is a target for SENP1-catalyzed deSUMOylation in normoxic cells, we expressed FLAG-tagged wild-type BHLHE40 or a described SUMOylation-deficient mutant in the above-mentioned His-SUMO1 expressing cells (Hong et al., 2011; Wang et al., 2012). Cells were either mock depleted or depleted from SENP1 by siRNA, and after cells lysis, His-SUMO1 conjugates were captured on Ni-NTA beads. Recovered material, as well as an aliquot of the input, was probed by anti-FLAG antibodies (Figure 4C). In input material, a 55 kDa FLAG-BHLHE40 species was detected in all samples. However, in SENP1-depleted cells, an additional 70 kDa form corresponding to the His-SUMO1-BHLHE40 conjugate was specifically enriched on Ni-NTA beads in cells expressing wild-type BHLHE40 but not the SUMOylation-deficient mutant (Figure 4C). These data support the idea that BHLHE40 is a SENP1-regulated SUMO1 target, with K159 and K279 serving as the major SUMO attachment sites. BHLHE40 was previously described as a negative regulator of PGC-1α expression (LaGory et al., 2015). To analyze whether SUMOylation of BHLHE40 has the potential to affect this process, we performed reporter gene assays on a luciferase reporter that contains the promoter region of the PGC-1α gene. In this experimental setup, the repressive potential of wild-type BHLHE40 was higher than the repression by the SUMOylation-deficient mutant (Figure 4D). Although the differences were moderate, we found that compared to wild-type BHLHE40, we consistently needed to double the amount of plasmid encoding the BHLHE40 mutant to achieve comparable repression. Typically, relative luciferase activity was reduced to 40% upon transfection of 200 ng of a plasmid encoding wild-type BHLHE40. To reach this extend of inhibition, 400 ng of the plasmid encoding BHLHE40^{K159,279R} was required. The reduced repressive potential of the SUMO-deficient BHLHE40 variant might be due to reduced protein stability, because immunoblotting of corresponding cell extracts consistently revealed lower steady-state levels of the mutant. Altogether, these data provide evidence that BHLHE40 is a hypoxic SUMO target and further suggest that SUMOylation under hypoxia may enhance its stability and repressive potential.

DISCUSSION

Balanced SUMO conjugation and deconjugation is an important way to control cellular signaling pathways and protein networks. SENPs are well-established key enzymes for SUMO deconjugation. However, the physiological stimuli controlling SENP activity are largely unknown. Here we show that hypoxia induces a rapid and reversible inhibition of SENP1 and SENP3, thereby triggering alterations in SUMO modification of a set of cellular proteins.

The physiological consequence of enhanced SUMOylation in hypoxia is not entirely clear, but several lines of evidence suggest that the SUMO system exerts a protective function in hypoxia. The strong increase in SUMO conjugation observed in mouse models of cerebral or cardiac ischemia, as well as in cellular models of ischemia, is mainly regarded as a tolerance mechanism against hypoxia (Guo et al., 2013; Loftus et al., 2009; Yang et al., 2008). Our proteomic data support the idea that hypoxia-induced SUMOylation facilitates metabolic adaptations in hypoxia, which are characterized by the inhibition of mitochondrial aerobic metabolism and the activation of anaerobic glycolysis. The transcription factor BHLHE40 (Stra13/DEC1) that we find hyperSUMOylated in hypoxia contributes to the inhibitory effect of hypoxia on mitochondrial aerobic metabolism through repression of genes involved in oxidative metabolism (Kato et al., 2014). One key target of BHLHE40 in this pathway is the metabolic master regulator PGC-1α (Chung et al., 2015; LaGory et al., 2015). We show that SUMOylation of BHLHE40 enhances its repressive potential on a PGC-1α luciferase reporter gene, suggesting that its hypoxic SUMOylation amplifies the inhibition of PGC-1α expression. It has already

Figure 4. Hypoxic SUMOylation of the Transcriptional Co-repressor BHLHE40

(A) A denaturing SUMO1 IP was performed from normoxic or hypoxic (24 hr) HeLa cell lysates. Input and immunopurified material was analyzed by immunoblotting against BHLHE40.

(B) Denaturing Ni-NTA pull-down was performed in HeLa cells expressing His-SUMO1 from a Tet-inducible promoter. Cell lysates (±Dox induction) from normoxic and hypoxic cells were used to monitor BHLHE40 and His-SUMO1. Input (left side) and pull-down (right side) were probed for BHLHE40 (upper panels) and His-SUMO1 (lower panels). To probe for His-SUMO1 in the Ni-NTA pull-down, only one-tenth of the recovered material was loaded. The asterisks in the input mark an unspecific band detected by the BHLHE40 antibody when cells are lysed in Ni-NTA lysis buffer.

(C) HeLa cells were transfected with control siRNA or siRNA directed against SENP1, and 24 hr later, wild-type BHLHE40 or the SUMO-deficient variant BHLHE40^{K159R,K279R} was expressed. After denaturing cell lysis and Ni-NTA pull-down, samples were stained against FLAG-tagged BHLHE40 (upper panels) or His-SUMO1 (lower panel). The left panels show input samples; the right panels show samples after pull-down. The His-SUMO1-BHLHE40 conjugate is specifically enriched upon Ni-NTA pull-down, while nonSUMOylated FLAG-BHLHE40 is present in all samples due to its high abundance.

(D) Dual-luciferase reporter assay was performed on a luciferase reporter gene containing the PGC-1α promoter. Cells were transfected with the indicated plasmids. Data show the average (±SEM) from at least four independent experiments. The p values are given. The immunoblot shows the expression of FLAG-BHLHE40 or FLAG-BHLHE40^{K159R,K279R} in a representative experiment, together with the anti-vinculin loading control.

been reported that SUMO conjugation to BHLHE40 promotes its ability to transcriptionally repress cyclin D1 or CLOCK/BMAL1-mediated transcriptional activity (Hong et al., 2011; Wang et al., 2012). The consistent, but relatively moderate, contribution of SUMOylation to the repressive effect of BHLHE40 observed in reporter gene assays can be explained by SUMO-mediated targeting of multiple components within transcriptional complexes (Jentsch and Psakhye, 2013; Raman et al., 2013). SUMOylation of PGC-1α was reported to attenuate its transcriptional activity, and deSUMOylation of PGC-1α by SENP1 was proposed to regulate mitochondrial biogenesis and activity (Cai et al., 2012). We provide compelling evidence that BHLHE40 is a target for SENP1-mediated deSUMOylation. We therefore propose a pathway in which hypoxic inhibition of SENP1 triggers SUMOylation of BHLHE40 and possibly other transcriptional regulators, including PCG-1α, to counter PGC-1α induction of mitochondrial activity. It has been proposed that SUMO modification of BHLHE40 may either facilitate recruitment of histone deacetylases (HDACs) or promote the stability of BHLHE40 (Hong et al., 2011; Wang et al., 2012). Our data are in agreement with the latter possibility, because we consistently detect a lower steady-state level of the SUMO-deficient variant $BHLHE40^{K159R,K279R}$ when compared to wild-type BHLHE40. We are investigating the underlying mechanism.

Hypoxic SUMOylation of BHLHE40 may therefore contribute to the inhibition of mitochondrial aerobic metabolism. Enhanced SUMOylation of glucose transporter GLUT1 (SLC2A1) that is found in hypoxia may in turn facilitate anaerobic glycolysis by stimulating cellular glucose uptake, because an increase in glucose uptake and glycolytic flux has been demonstrated upon SUMO1 overexpression in mammalian cells (Agbor et al., 2011). Moreover, overexpression of SENP2 reduces glucose uptake and lactate production, supporting the critical role of the SUMO system in reprogramming cellular glucose metabolism (Tang et al., 2013). How the altered SUMOylation of other candidate targets is connected to hypoxic signaling remains to be determined, but the enrichment of transcriptional repressors among the hyperSUMOylated proteins points to a role for SUMO in the coordination of hypoxic gene expression programs. Hypoxia also has been shown to redirect Ubc9 to distinct transcription factors, thus limiting their transcriptional activity by enhanced SUMOylation (Hsieh et al., 2013).

Our study provides a proteome-wide dataset of hypoxic SUMOylation in mammalian cells. A comparison of our dataset with published proteomics on altered SUMO3 conjugation upon transient oxygen and glucose deprivation reveals some common candidates (Yang et al., 2012). Among the 22 upregulated SUMO targets identified by Yang et al. (2012), PIAS2, IRF2BP1, and PML were found in our study. Moreover, the related co-repressors NAB1/2 were found in both studies. In addition, in both studies, RSF1 and BRD8 were found to be downregulated upon hypoxia or ischemia. The limited overlap of both studies can be explained by several facts. First, Yang et al. (2012) used a neuroblastoma cell line stably expressing HA-tagged SUMO3, while we enriched for proteins conjugated to endogenous SUMO1. Second, in the work by Yang et al. (2012), proteomics was performed upon 6 hr of oxygen and glucose deprivation followed by 30 min of reoxygenation, which is different from our experimental setup. Despite these differences, it will be important to investigate whether the aforementioned regulators are core factors of a common hypoxic or ischemic SUMO response.

Our data support the idea that the inactivation of SENPs triggers the accumulation of SUMO conjugates in hypoxia. Consistent with our findings, data from SENP1 knockout mice indicate that SENP1 is the primary activity for deSUMOylation of SUMO1-modified proteins (Sharma et al., 2013). Although the balance of SUMO conjugation and deconjugation in hypoxia is likely regulated at multiple layers (Carbia-Nagashima et al., 2007), our data suggest that the inactivation of SENP1 is significantly contributing to the enrichment of SUMO1 conjugates. The subset of SUMO targets that are deconjugated by SENP1 has not yet been defined, but an emerging concept is that specific SENPs counterbalance SUMOylation of a whole set of targets that are functionally or physically connected to one another (Jentsch and Psakhye, 2013). Notably, earlier work defined HIF1α as target for SENP1 and proposed that SENP1-mediated deSUMOylation contributes to HIF1α stabilization in hypoxia (Cheng et al., 2007). Although we did not detect HIF1α in our proteomic screen, the hypoxic inactivation of SENP1 may act as a feedback mechanism to limit HIF1α accumulation in prolonged hypoxia.

Only a subset of SUMO1 targets is affected in its SUMOylation by hypoxia. RanGAP1, the key example of a target with a slow turnover of SUMOylation, does not exhibit altered modification in hypoxia. By contrast, the dynamic autoSUMOylation of the E3 SUMO ligases PIAS2 and RanBP2 is highly sensitive to SENP inhibition. While the accumulation of SUMO1 conjugates is significant, the overall increase in SUMO2 conjugates is limited. A possible explanation could be that SENPs, including SENP1 and SENP3, function not only in deconjugation but also in processing of the SUMO2/3 precursors. A reduction in their activity therefore does not always lead to the accumulation of conjugates and may even reduce modification due to the limited availability of conjugatable, processed SUMO2/3. This can explain why, in our proteomic approach, a subset of SUMO targets is not significantly enriched in hypoxia or even decreased. Alternatively, hyperSUMOylation of some targets can lead to proteasomal degradation by the StUbL (SUMO-targeted ubiquitin ligase) pathway (Sriramachandran and Dohmen, 2014). Considering that the StUbL pathway is triggered by SUMO chains, we find SUMO2/3 in the SUMO1 immunoprecipitates, indicating that we also enriched for mixed SUMO1-SUMO2/3 chains. The amount of immunopurified SUMO2 was reduced 4-fold in hypoxia compared to normoxia, which is in line with the idea that these mixed chains are prone to proteolytic degradation. Some targets with reduced hypoxic SUMOylation are found at lower protein levels in hypoxic versus normoxic cells. Whether this is due to SUMO-dependent turnover or transcriptional repression in hypoxia remains to be determined.

The mechanistic basis for the rapid and reversible inactivation of SENP1/3 in hypoxia is unclear, but it is tempting to speculate that changes in the cellular redox state may act as a switch for activation and deactivation of SENPs. One possible mechanism could be the oxidation of catalytic cysteine residues by reactive oxygen species (ROS), which is a well-established mechanism for the reversible inactivation of deubiquitinases

(Cotto-Rios et al., 2012; Kulathu et al., 2013). In hypoxic cells, ROS is mainly generated in mitochondria, but the perinuclear clustering of mitochondria in hypoxic cells was proposed to preferentially trigger the accumulation of nuclear ROS (Al-Mehdi et al., 2012; Murphy, 2012). As primarily nuclear proteins, SENP1 and SENP3 may thus be particularly vulnerable for oxidation. SENP1 is enriched at the nuclear pore and thus would be directly exposed to perinuclear ROS. For both SENP1 and SENP3, there is evidence that the catalytic cysteine residue undergoes oxidation when cells are directly exposed to hydrogen peroxide (Xu et al., 2008; Yang et al., 2014). Alternatively, alterations in the balance between reduced (glutathione [GSH]) and oxidized (glutathione disulfide [GSSG]) glutathione due to hypoxic depletion of nicotinamide adenine dinucleotide phosphate (NADPH) could contribute to oxidative inactivation of SENPs. In line with this idea, recent work has connected SENP1 activity to the cellular GSSG/GSH balance (Attie, 2015; Ferdaoussi et al., 2015).

Altogether, the oxygen-sensitive control of SENP activity provides important insight into the regulation of this enzyme family. Hypoxic inactivation of SENP family members may also be important in the context of human disease, because it may help oxygen-deprived tissues to adapt to a hypoxic environment.

EXPERIMENTAL PROCEDURES

Cell Culture and Transfection

HeLa cells were cultured under standard conditions. The cell line stably expressing His-SUMO1 from a tetracycline-inducible promoter has been described (Ullmann et al., 2012). Hypoxic incubations were performed in a hypoxic workstation with 1% O_2, 94% N_2, and 5% CO_2 (Invivo2 400, Ruskinn Technology) at 37°C for the indicated times. To avoid reoxygenation of hypoxic cells, samples were harvested within the hypoxic chamber. For siRNA knockdown experiments, HeLa cells were transfected twice within 5 days using the Lipofectamine RNAiMAX transfection reagent (Thermo Fisher Scientific) according to the manufacturer's instructions. On day 1, cells were seeded and reverse transfected with a total of 250 pmol of siRNA per 60 mm dish. On day 3, the procedure was repeated. Sequences of siRNAs are listed in Supplemental Experimental Procedures.

SDS-PAGE, Western Blotting, and Ni-NTA Pull-Down

SDS-PAGE and western blotting was done by standard procedures. Ni-NTA pull-down was done as previously described (Ullmann et al., 2012). Antibodies are listed in Supplemental Experimental Procedures.

qRT-PCR and Luciferase Reporter Gene Assays

Luciferase reporter gene assays and qRT-PCR experiments were done as previously described (Nayak et al., 2014; Ullmann et al., 2012).

Measuring SUMO Protease Activity by SUMO1-AMC or SUMO2-AMC Cleavage Assays and SUMO1-VS or SUMO2-VS Adduct Formation

SUMO protease activity in total HeLa cell lysates was determined by using SUMO1- or SUMO2-AMC or SUMO1-VS or SUMO2-VS as substrate, as detailed in Supplemental Experimental Procedures.

Enrichment of SUMO1 Conjugates by Immunopurification and MS

To enrich for endogenous SUMO1 targets, we followed a recently published procedure (Barysch et al., 2014; Becker et al., 2013). For each anti-SUMO1 and IgG control IP in normoxia and hypoxia, 13 mg of protein from HeLa cell lysates were used. Enriched SUMO1 targets and normoxic or hypoxic protein lysates (30 μg) were subjected to in-gel digestion. Proteins were separated according their molecular weight by subjecting them to SDS-PAGE (4%–12% NuPage BisTris Gel, Invitrogen) followed by Colloidal blue staining (Expedeon). Gel lanes were cut into equal pieces and digested in the gel as described by Shevchenko et al. (2006) and as detailed in Supplemental Experimental Procedures. Collected peptide mixtures were concentrated and desalted using the stop and go extraction (STAGE) technique (Rappsilber et al., 2003).

Liquid Chromatography-Mass Spectrometry and Data Analysis

Details on liquid chromatography-mass spectrometry (LC-MS) and data analysis are found in Supplemental Experimental Procedures. In brief, all experiments were done on a Q Exactive HF benchtop mass spectrometer (Michalski et al., 2011). For data analysis, all acquired raw files were processed using MaxQuant (v.1.5.3.12) (Cox and Mann, 2008) and the implemented Andromeda search engine (Cox et al., 2011). Relative label-free quantification of proteins was done using the MaxLFQ algorithm integrated into MaxQuant (Cox et al., 2014).

SUPPLEMENTAL INFORMATION

Supplemental Information includes Supplemental Experimental Procedures, five figures, and one table and can be found with this article online at http://dx.doi.org/10.1016/j.celrep.2016.08.031.

AUTHOR CONTRIBUTIONS

K.K. and K.W. conducted the experiments, L.M. and N.D. gave critical experimental advice, S.H. performed the MS and analyzed the MS data, and S.M. supervised the project and wrote the manuscript. K.K. and S.H. compiled the figures.

ACKNOWLEDGMENTS

This work was funded by the DFG collaborative research centers (SFB815 and SFB1177), LOEWE Ub-Net initiative, and DFG MU (1764, 4-1).

Received: February 16, 2016
Revised: July 13, 2016
Accepted: August 9, 2016
Published: September 13, 2016

REFERENCES

Agbor, T.A., Cheong, A., Comerford, K.M., Scholz, C.C., Bruning, U., Clarke, A., Cummins, E.P., Cagney, G., and Taylor, C.T. (2011). Small ubiquitin-related modifier (SUMO)-1 promotes glycolysis in hypoxia. J. Biol. Chem. *286*, 4718–4726.

Al-Mehdi, A.B., Pastukh, V.M., Swiger, B.M., Reed, D.J., Patel, M.R., Bardwell, G.C., Pastukh, V.V., Alexeyev, M.F., and Gillespie, M.N. (2012). Perinuclear mitochondrial clustering creates an oxidant-rich nuclear domain required for hypoxia-induced transcription. Sci. Signal. *5*, ra47.

Attie, A.D. (2015). How do reducing equivalents increase insulin secretion? J. Clin. Invest. *125*, 3754–3756.

Barysch, S.V., Dittner, C., Flotho, A., Becker, J., and Melchior, F. (2014). Identification and analysis of endogenous SUMO1 and SUMO2/3 targets in mammalian cells and tissues using monoclonal antibodies. Nat. Protoc. *9*, 896–909.

Becker, J., Barysch, S.V., Karaca, S., Dittner, C., Hsiao, H.H., Berriel Diaz, M., Herzig, S., Urlaub, H., and Melchior, F. (2013). Detecting endogenous SUMO targets in mammalian cells and tissues. Nat. Struct. Mol. Biol. *20*, 525–531.

Cai, R., Yu, T., Huang, C., Xia, X., Liu, X., Gu, J., Xue, S., Yeh, E.T., and Cheng, J. (2012). SUMO-specific protease 1 regulates mitochondrial biogenesis through PGC-1α. J. Biol. Chem. *287*, 44464–44470.

Carbia-Nagashima, A., Gerez, J., Perez-Castro, C., Paez-Pereda, M., Silberstein, S., Stalla, G.K., Holsboer, F., and Arzt, E. (2007). RSUME, a small RWD-containing protein, enhances SUMO conjugation and stabilizes HIF-1alpha during hypoxia. Cell *131*, 309–323.

Cheng, J., Kang, X., Zhang, S., and Yeh, E.T. (2007). SUMO-specific protease 1 is essential for stabilization of HIF1alpha during hypoxia. Cell *131*, 584–595.

Chung, S.Y., Kao, C.H., Villarroya, F., Chang, H.Y., Chang, H.C., Hsiao, S.P., Liou, G.G., and Chen, S.L. (2015). Bhlhe40 represses PGC-1α activity on metabolic gene promoters in myogenic cells. Mol. Cell. Biol. *35*, 2518–2529.

Cimarosti, H., Ashikaga, E., Jaafari, N., Dearden, L., Rubin, P., Wilkinson, K.A., and Henley, J.M. (2012). Enhanced SUMOylation and SENP-1 protein levels following oxygen and glucose deprivation in neurones. J. Cereb. Blood Flow Metab. *32*, 17–22.

Cotto-Rios, X.M., Békés, M., Chapman, J., Ueberheide, B., and Huang, T.T. (2012). Deubiquitinases as a signaling target of oxidative stress. Cell Rep. *2*, 1475–1484.

Cox, J., and Mann, M. (2008). MaxQuant enables high peptide identification rates, individualized p.p.b.-range mass accuracies and proteome-wide protein quantification. Nat. Biotechnol. *26*, 1367–1372.

Cox, J., Neuhauser, N., Michalski, A., Scheltema, R.A., Olsen, J.V., and Mann, M. (2011). Andromeda: a peptide search engine integrated into the MaxQuant environment. J. Proteome Res. *10*, 1794–1805.

Cox, J., Hein, M.Y., Luber, C.A., Paron, I., Nagaraj, N., and Mann, M. (2014). Accurate proteome-wide label-free quantification by delayed normalization and maximal peptide ratio extraction, termed MaxLFQ. Mol. Cell. Proteomics *13*, 2513–2526.

Ferdaoussi, M., Dai, X., Jensen, M.V., Wang, R., Peterson, B.S., Huang, C., Ilkayeva, O., Smith, N., Miller, N., Hajmrle, C., et al. (2015). Isocitrate-to-SENP1 signaling amplifies insulin secretion and rescues dysfunctional β cells. J. Clin. Invest. *125*, 3847–3860.

Flotho, A., and Melchior, F. (2013). Sumoylation: a regulatory protein modification in health and disease. Annu. Rev. Biochem. *82*, 357–385.

Gareau, J.R., and Lima, C.D. (2010). The SUMO pathway: emerging mechanisms that shape specificity, conjugation and recognition. Nat. Rev. Mol. Cell Biol. *11*, 861–871.

Guo, C., Hildick, K.L., Luo, J., Dearden, L., Wilkinson, K.A., and Henley, J.M. (2013). SENP3-mediated deSUMOylation of dynamin-related protein 1 promotes cell death following ischaemia. EMBO J. *32*, 1514–1528.

Hickey, C.M., Wilson, N.R., and Hochstrasser, M. (2012). Function and regulation of SUMO proteases. Nat. Rev. Mol. Cell Biol. *13*, 755–766.

Hong, Y., Xing, X., Li, S., Bi, H., Yang, C., Zhao, F., Liu, Y., Ao, X., Chang, A.K., and Wu, H. (2011). SUMOylation of DEC1 protein regulates its transcriptional activity and enhances its stability. PLoS ONE *6*, e23046.

Hsieh, Y.L., Kuo, H.Y., Chang, C.C., Naik, M.T., Liao, P.H., Ho, C.C., Huang, T.C., Jeng, J.C., Hsu, P.H., Tsai, M.D., et al. (2013). Ubc9 acetylation modulates distinct SUMO target modification and hypoxia response. EMBO J. *32*, 791–804.

Huang, C., Han, Y., Wang, Y., Sun, X., Yan, S., Yeh, E.T., Chen, Y., Cang, H., Li, H., Shi, G., et al. (2009). SENP3 is responsible for HIF-1 transactivation under mild oxidative stress via p300 de-SUMOylation. EMBO J. *28*, 2748–2762.

Huang, C.J., Wu, D., Khan, F.A., and Huo, L.J. (2015). DeSUMOylation: an important therapeutic target and protein regulatory event. DNA Cell Biol. *34*, 652–660.

Jentsch, S., and Psakhye, I. (2013). Control of nuclear activities by substrate-selective and protein-group SUMOylation. Annu. Rev. Genet. *47*, 167–186.

Kato, Y., Kawamoto, T., Fujimoto, K., and Noshiro, M. (2014). DEC1/STRA13/SHARP2 and DEC2/SHARP1 coordinate physiological processes, including circadian rhythms in response to environmental stimuli. Curr. Top. Dev. Biol. *110*, 339–372.

Kenneth, N.S., and Rocha, S. (2008). Regulation of gene expression by hypoxia. Biochem. J. *414*, 19–29.

Kolli, N., Mikolajczyk, J., Drag, M., Mukhopadhyay, D., Moffatt, N., Dasso, M., Salvesen, G., and Wilkinson, K.D. (2010). Distribution and paralogue specificity of mammalian deSUMOylating enzymes. Biochem. J. *430*, 335–344.

Kulathu, Y., Garcia, F.J., Mevissen, T.E., Busch, M., Arnaudo, N., Carroll, K.S., Barford, D., and Komander, D. (2013). Regulation of A20 and other OTU deubiquitinases by reversible oxidation. Nat. Commun. *4*, 1569.

Kuo, M.L., den Besten, W., Thomas, M.C., and Sherr, C.J. (2008). Arf-induced turnover of the nucleolar nucleophosmin-associated SUMO-2/3 protease Senp3. Cell Cycle *7*, 3378–3387.

LaGory, E.L., Wu, C., Taniguchi, C.M., Ding, C.K., Chi, J.T., von Eyben, R., Scott, D.A., Richardson, A.D., and Giaccia, A.J. (2015). Suppression of PGC-1α is critical for reprogramming oxidative metabolism in renal cell carcinoma. Cell Rep. *12*, 116–127.

Lima, C.D., and Reverter, D. (2008). Structure of the human SENP7 catalytic domain and poly-SUMO deconjugation activities for SENP6 and SENP7. J. Biol. Chem. *283*, 32045–32055.

Loftus, L.T., Gala, R., Yang, T., Jessick, V.J., Ashley, M.D., Ordonez, A.N., Thompson, S.J., Simon, R.P., and Meller, R. (2009). Sumo-2/3-ylation following in vitro modeled ischemia is reduced in delayed ischemic tolerance. Brain Res. *1272*, 71–80.

Madu, I.G., and Chen, Y. (2012). Assays for investigating deSUMOylation enzymes. Curr. Protoc. Mol. Biol. *99*, 10 30.1–10.30.13.

Michalski, A., Damoc, E., Hauschild, J.P., Lange, O., Wieghaus, A., Makarov, A., Nagaraj, N., Cox, J., Mann, M., and Horning, S. (2011). Mass spectrometry-based proteomics using Q Exactive, a high-performance benchtop quadrupole Orbitrap mass spectrometer. Mol. Cell. Proteomics *10*, 1–12.

Mukhopadhyay, D., and Dasso, M. (2007). Modification in reverse: the SUMO proteases. Trends Biochem. Sci. *32*, 286–295.

Murphy, M.P. (2012). Modulating mitochondrial intracellular location as a redox signal. Sci. Signal. *5*, pe39.

Nayak, A., and Müller, S. (2014). SUMO-specific proteases/isopeptidases: SENPs and beyond. Genome Biol. *15*, 422.

Nayak, A., Viale-Bouroncle, S., Morsczeck, C., and Muller, S. (2014). The SUMO-specific isopeptidase SENP3 regulates MLL1/MLL2 methyltransferase complexes and controls osteogenic differentiation. Mol. Cell *55*, 47–58.

Raman, N., Nayak, A., and Muller, S. (2013). The SUMO system: a master organizer of nuclear protein assemblies. Chromosoma *122*, 475–485.

Rappsilber, J., Ishihama, Y., and Mann, M. (2003). Stop and go extraction tips for matrix-assisted laser desorption/ionization, nanoelectrospray, and LC/MS sample pretreatment in proteomics. Anal. Chem. *75*, 663–670.

Reverter, D., and Lima, C.D. (2004). A basis for SUMO protease specificity provided by analysis of human Senp2 and a Senp2-SUMO complex. Structure *12*, 1519–1531.

Reverter, D., and Lima, C.D. (2006). Structural basis for SENP2 protease interactions with SUMO precursors and conjugated substrates. Nat. Struct. Mol. Biol. *13*, 1060–1068.

Semenza, G.L. (2014). Oxygen sensing, hypoxia-inducible factors, and disease pathophysiology. Annu. Rev. Pathol. *9*, 47–71.

Sharma, P., Yamada, S., Lualdi, M., Dasso, M., and Kuehn, M.R. (2013). Senp1 is essential for desumoylating Sumo1-modified proteins but dispensable for Sumo2 and Sumo3 deconjugation in the mouse embryo. Cell Rep. *3*, 1640–1650.

Shen, L., Tatham, M.H., Dong, C., Zagórska, A., Naismith, J.H., and Hay, R.T. (2006a). SUMO protease SENP1 induces isomerization of the scissile peptide bond. Nat. Struct. Mol. Biol. *13*, 1069–1077.

Shen, L.N., Dong, C., Liu, H., Naismith, J.H., and Hay, R.T. (2006b). The structure of SENP1-SUMO-2 complex suggests a structural basis for discrimination between SUMO paralogues during processing. Biochem. J. *397*, 279–288.

Shevchenko, A., Tomas, H., Havlis, J., Olsen, J.V., and Mann, M. (2006). In-gel digestion for mass spectrometric characterization of proteins and proteomes. Nat. Protoc. *1*, 2856–2860.

Sriramachandran, A.M., and Dohmen, R.J. (2014). SUMO-targeted ubiquitin ligases. Biochim. Biophys. Acta *1843*, 75–85.

Tang, S., Huang, G., Tong, X., Xu, L., Cai, R., Li, J., Zhou, X., Song, S., Huang, C., and Cheng, J. (2013). Role of SUMO-specific protease 2 in reprogramming cellular glucose metabolism. PLoS ONE *8*, e63965.

Ullmann, R., Chien, C.D., Avantaggiati, M.L., and Muller, S. (2012). An acetylation switch regulates SUMO-dependent protein interaction networks. Mol. Cell *46*, 759–770.

Wang, Y., Rao, V.K., Kok, W.K., Roy, D.N., Sethi, S., Ling, B.M., Lee, M.B., and Taneja, R. (2012). SUMO modification of Stra13 is required for repression of cyclin D1 expression and cellular growth arrest. PLoS ONE *7*, e43137.

Wilkinson, K.A., and Henley, J.M. (2010). Mechanisms, regulation and consequences of protein SUMOylation. Biochem. J. *428*, 133–145.

Wilkinson, K.D., Gan-Erdene, T., and Kolli, N. (2005). Derivitization of the C-terminus of ubiquitin and ubiquitin-like proteins using intein chemistry: methods and uses. Methods Enzymol. *399*, 37–51.

Xu, Z., Chau, S.F., Lam, K.H., Chan, H.Y., Ng, T.B., and Au, S.W. (2006). Crystal structure of the SENP1 mutant C603S-SUMO complex reveals the hydrolytic mechanism of SUMO-specific protease. Biochem. J. *398*, 345–352.

Xu, Z., Lam, L.S., Lam, L.H., Chau, S.F., Ng, T.B., and Au, S.W. (2008). Molecular basis of the redox regulation of SUMO proteases: a protective mechanism of intermolecular disulfide linkage against irreversible sulfhydryl oxidation. FASEB J. *22*, 127–137.

Yan, S., Sun, X., Xiang, B., Cang, H., Kang, X., Chen, Y., Li, H., Shi, G., Yeh, E.T., Wang, B., et al. (2010). Redox regulation of the stability of the SUMO protease SENP3 via interactions with CHIP and Hsp90. EMBO J. *29*, 3773–3786.

Yang, J., Gupta, V., Carroll, K.S., and Liebler, D.C. (2014). Site-specific mapping and quantification of protein S-sulphenylation in cells. Nat. Commun. *5*, 4776.

Yang, W., Sheng, H., Warner, D.S., and Paschen, W. (2008). Transient global cerebral ischemia induces a massive increase in protein sumoylation. J. Cereb. Blood Flow Metab. *28*, 269–279.

Yang, W., Thompson, J.W., Wang, Z., Wang, L., Sheng, H., Foster, M.W., Moseley, M.A., and Paschen, W. (2012). Analysis of oxygen/glucose-deprivation-induced changes in SUMO3 conjugation using SILAC-based quantitative proteomics. J. Proteome Res. *11*, 1108–1117.

Yeh, E.T. (2009). SUMOylation and de-SUMOylation: wrestling with life's processes. J. Biol. Chem. *284*, 8223–8227.

Cell Reports, Volume *16*

Supplemental Information

SUMO Signaling by Hypoxic Inactivation of SUMO-Specific Isopeptidases

Kathrin Kunz, Kristina Wagner, Luca Mendler, Soraya Hölper, Nathalie Dehne, and Stefan Müller

Supplemental Material

Supplemental Material & Methods

siRNAs, Primers and Antibodies

The following siRNAs were used:
Control: CGU ACG CGG AAU ACU UCG AdTdT
SENP1: AUU CAG UAC AUG AUU CAG UdTdT
SENP3: ACG UGG ACA UCU UCA AUA AdTdT

The following primers were used for RT-qPCR:
SUMO1: TTCAACTGAGGACTTGGGGG; TGGAACACCCTGTCTTTGAC
SUMO2: GCCGACGAAAAGCCCAAGG; TGACAATCCCTGTCGTTCACAA
SUMO3: CCCAAGGAGGGTGTGAAGAC; ATTGACAAGCCCTGCCTCTC
TBP: GGGCCGCCGGCTGTTTAACT; AGCCCTGAGCGTAAGGTGGCA

The following antibodies were used for Western Blotting and immunoprecipitation:
anti-SENP1 (clone D1607,Cell signaling), anti-SENP3 (clone D20A10, Cell signaling), anti-SENP5 (ABdIN459856, Antibodies-online), anti-SENP6 (HPAA024376, Sigma-Aldrich), anti-SUMO1 (GMP1, Clone 21C7, Invitrogen), anti-SUMO2/3 (clone 1E7, M114-3, MBL), anti-HA (clone 16B12, Covance), anti-β-Tubulin (clone E7, Developmental Studies Hybridoma Bank), anti-HIF1α (Novus), anti-BHLHE40 (Dec1, Bethyl, A300-649-M), RGS-His (Qiagen).

Determining SUMO protease activity by SUMO1/2-AMC cleavage assays

SUMO protease activity in total HeLa cell lysates was determined by using SUMO1-AMC or SUMO2-AMC as substrate. HeLa cells were cultured under normal conditions or in hypoxia. To prepare lysates, cells were washed three times with PBS, lysed in SEM buffer (0.25 mM sucrose, 20 mM MOPS, 1 mM EDTA, pH = 7.2, 1 mM DTT and protease inhibitor cocktail). For negative control samples 10 mM NEM was added. Protein concentration was determined by Biorad protein assay and either 7.5 µg or 14 µg of cell extract

were incubated with 500 ng of SUMO1-AMC (Enzo Life Sciences) or SUMO2-AMC (Boston Biochem) in the presence of activity assay buffer (50 mM Tris/HCl pH 7.5, 0.1 mg/ml BSA, 10 mM DTT). The measurement was carried out in black 384 well plates in a total volume of 50 µl. Fluorescence at λ_{ex} 380 nm and λ_{em} 460 nm was measured by Synergy H1 plate reader using Gen5 software.

Determining SUMO protease activity by SUMO1/2-VS adduct formation

100 µg of total HeLa cell extracts prepared in SEM buffer were incubated with 50 ng of either SUMO1-VS or SUMO2-VS (Boston Biochem) for 15 min at 25 °C. The reaction was stopped by addition of SDS-PAGE sample buffer (5 min, 95 °C).

Western blotting was done against different SENPs or the HA-tag.

Trypsin digestion for mass spectrometry

For in gel digestion gel lanes were cut into equal pieces and digested in the gel as described by Shevchenko et al. (Shevchenko et al., 2006). In brief, gel pieces were washed, destained and dehydrated. Proteins were reduced with 10 mM dithiothreitol (DTT), alkylated with 55 mM iodoacetamide (IAA) and digested with the endopeptidase sequencing-grade Trypsin (Promega) overnight. Generated peptides were extracted using an increasing acetonitrile concentration. Collected peptide mixtures were concentrated and desalted using the Stop and Go Extraction (STAGE) technique (Rappsilber et al., 2003). For in solution digestion protein mixtures (20 µg) were precipitated overnight using 4 volumes of ice-cold acetone. The protein pellet was dissolved in 6 M urea, 2 M thiourea, 10 mM HEPES, pH 8 and subjected to digestion following reduction of disulfide bonds and alkylation as described above. For the first digestion step LysC (Wako) (protein to LysC ratio = 100:1) was added for 3 hours. Then, the samples were diluted to 2 M urea with 50 mM ammonium bicarbonate, and sequencing-grade trypsin (Promega, Madison, WI) was added to the samples (protein to trypsin ratio = 100:1) overnight at room temperature. Peptide mixtures were desalted as described above for in gel digestion.

Liquid chromatography and mass spectrometry

Instrumentation for LC-MS/MS analysis consisted of a NanoLC 1000 coupled via a nano-electrospray ionization source to the quadrupole-based Q Exactive HF benchtop mass spectrometer (Michalski et al., 2011). Peptide separation was carried out according to their hydrophobicity on an in-house packed 20 cm column with 1.9 mm C18 beads (Dr Maisch GmbH) using a binary buffer system consisting of solution A: 0.1% formic acid and B: 80% acetonitrile, 0.1% formic acid. 35 min / 75 min gradients were used for SUMO1-enriched and proteome samples, respectively. Linear gradients from 7–38% B in 20 min / 55 min were applied with a following increase to 95% B within 5 min /10 min and a re-equilibration to 5% B.

Q Exactive HF settings: MS spectra were acquired using 3E6 as an AGC target, a maximal injection time of 20 ms and a 60,000 / 15,000 resolution at 200 m/z for SUMO1-enriched and proteome samples. The mass spectrometer operated in a data dependent Top15 mode with subsequent acquisition of higher-energy collisional dissociation (HCD) fragmentation MS/MS spectra of the top 15 most intense peaks. Resolution for MS/MS spectra was set to 30,000 / 15,000 at 200m/z, AGC target to 1E5, max injection time to 64 ms / 25 ms and the isolation window to 1.8 Th / 2.2 Th.

Data Analysis

All acquired raw files were processed using MaxQuant (1.5.3.12) (Cox and Mann, 2008) and the implemented Andromeda search engine (Cox et al., 2011). For protein assignment, electrospray ionization-tandem mass spectrometry (ESI-MS/MS) fragmentation spectra were correlated with the Uniprot human database (v. 2015) including a list of common contaminants. Searches were performed with tryptic specifications and default settings for mass tolerances for MS and MS/MS spectra. Carbamidomethyl at cysteine residues was set as a fixed modification, while oxidation at methionine, acetylation at the N-terminus were defined as variable modifications. The minimal peptide length was set to seven amino acids, and the false discovery rate for proteins and peptide-spectrum matches to 1%. Relative lable-free quantification of proteins was done using the MaxLFQ algorithm integrated into MaxQuant (Cox et al., 2014). The minimum LFQ ratio count was set to 2

and the FastLFQ option was enabled. The match-between-run feature with a time window of 1 min was used. For further analysis, the Perseus software (1.5.0.31) was used and first filtered for contaminants and reverse entries as well as proteins that were only identified by a modified peptide. The LFQ intensities were logarithmized and grouped into triplicates. To overcome the missing value problem in immunoprecipitation data, proteins that were quantified less than 3 times in one of the experimental groups were discarded from further analysis. Then, missing values were imputed column-wise by a down-shifted (median-1.8) Gaussian distribution mimicking the detection limit of the mass spectrometer. Normal distribution was checked by visual histogram analysis.

Statistical methods used in luciferase activity assay

To test for statistical significance in luciferase reporter gene assays values from four independent experiments were used for calculation. The average values of firefly or renilla fluorescence were calculated and based on these average the ratio firefly/renilla was determined. Using the sample average, the ratio and the sample variance the standard error was calculated. A two-tailed Student’s t-distribution was performed, resulting in p-values < 0.05.

Legends to Supplemental Figures and Supplemental Figures

Supplemental Figure 1 related to Figure 1: Protein and mRNA levels of SUMO1, 2, 3 in normoxia and hypoxia

(A) MS-based proteome analysis was done for normoxic and hypoxic (24 hrs timepoint) HeLa cell lysates. Comparison of the log2 protein intensities after label free quantification for SUMO1, 2 or 3 in hypoxia and normoxia. (B) HeLa cells were cultured under normoxic or hypoxic conditions for indicated timepoints or reoxygenated for 30 minutes after 24 hours of hypoxia. SUMO1, SUMO2 or SUMO3 mRNA expression was quantified by RT-qPCR. Values represent the average of 2 independent experiments performed in triplicates (± SD) after normalization for TBP levels.

Supplemental Figure 2 related to Figure 2A-C: Hypoxia inhibits the catalytic activity of SUMO proteases

(A) HeLa cells were cultured under normoxic or hypoxic conditions for indicated times, cells were lysed in SDS-PAGE buffer and proteins separated by SDS-PAGE. Total cell lysates were blotted against SUMO1, SUMO2/3, HIF1α, SENP6, SENP3, SENP2, SENP1 and β -Tubulin as indicated. * indicates an unspecific band detected by anti-SENP1 antibody. (B) HeLa cells were lysed in SEM buffer and incubated with either HA-SUMO1-VS or HA-SUMO2-VS for 15 minutes at 25 °C. After separation of protein by SDS-PAGE immunoblotting was done anti-HA antibody. In lane 2 NEM was added to inhibit SUMO proteases. (C) HeLa lysate from control cells, hypoxic cells and hypoxic/reoxygenated cells (24 hrs hypoxia/30 min reoxygenation) were treated as in (B). Lysates were incubated with HA-SUMO1/2-VS probe and stained against HA. Top panel shows separation on a 7,5 % SDS-PAGE gel to detect higher molecular bands. For the middle panel and lower panel samples were applied on a 12,5 % gel to detect free HA-SUMO-VS probe and β-Tubulin, which served as loading control. NEM was added to the sample in lane 2 as negative control.

Supplemental Figure 3 related to Figure 2A-C: SENP activity in HeLa cells

Total HeLa cell extracts prepared in SEM buffer were incubated with or without HA-SUMO1/2-VS as indicated for 15 minutes at 25 °C. After separation by SDS-PAGE immunoblots were probed with anti-SENP1, anti-SENP2, anti-SENP5 or anti-SENP7 antibody. NEM was added as negative control where indicated. Anti-Tubulin immunoblot served as a loading control.

Supplemental Figure 4 related to Figure 3B, C: Quantitative MS in normoxic and hypoxic cells

(A) Principal component analysis showing high similarity among the triplicates. (B) Volcano plot depicting significantly enriched SUMO1-targets upon immunopurification of cellular proteins from normoxic cells under

denaturing conditions on anti-SUMO1 beads. Proteins with a 4-fold enrichment over IgG control and a p-value< 0.05 are indicated by red circles. For selected proteins gene names are given. Dashed line indicated FDR < 0.05. (C) Same as in B, but proteins immunopurified from hypoxic cells are shown.

Supplemental figure 5 related to Figure 4A: Hypoxic SUMOylation of the transcriptional co-repressor BHLHE40

Longer exposure of immunoblot shown in Figure 4A.

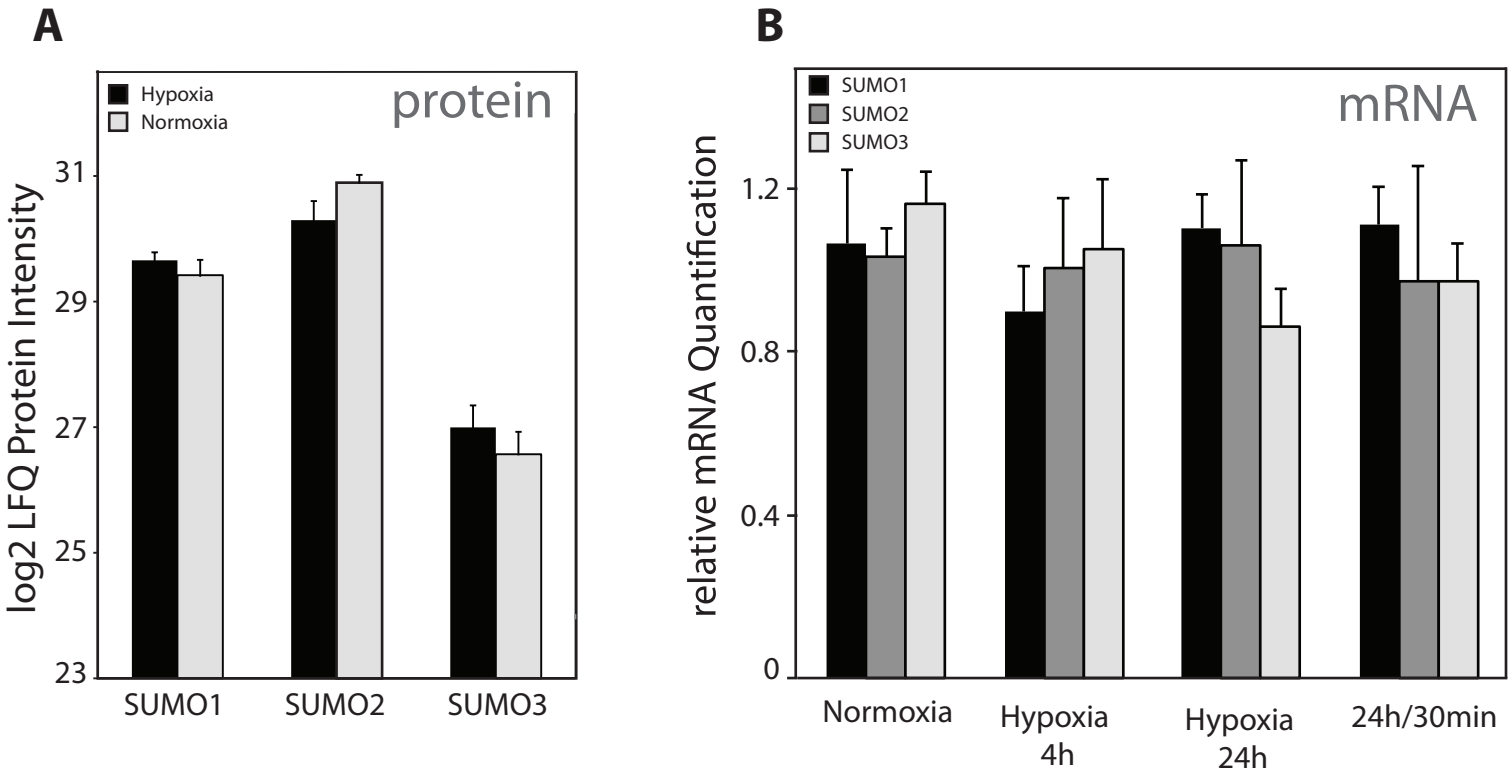

supplemental figure 1

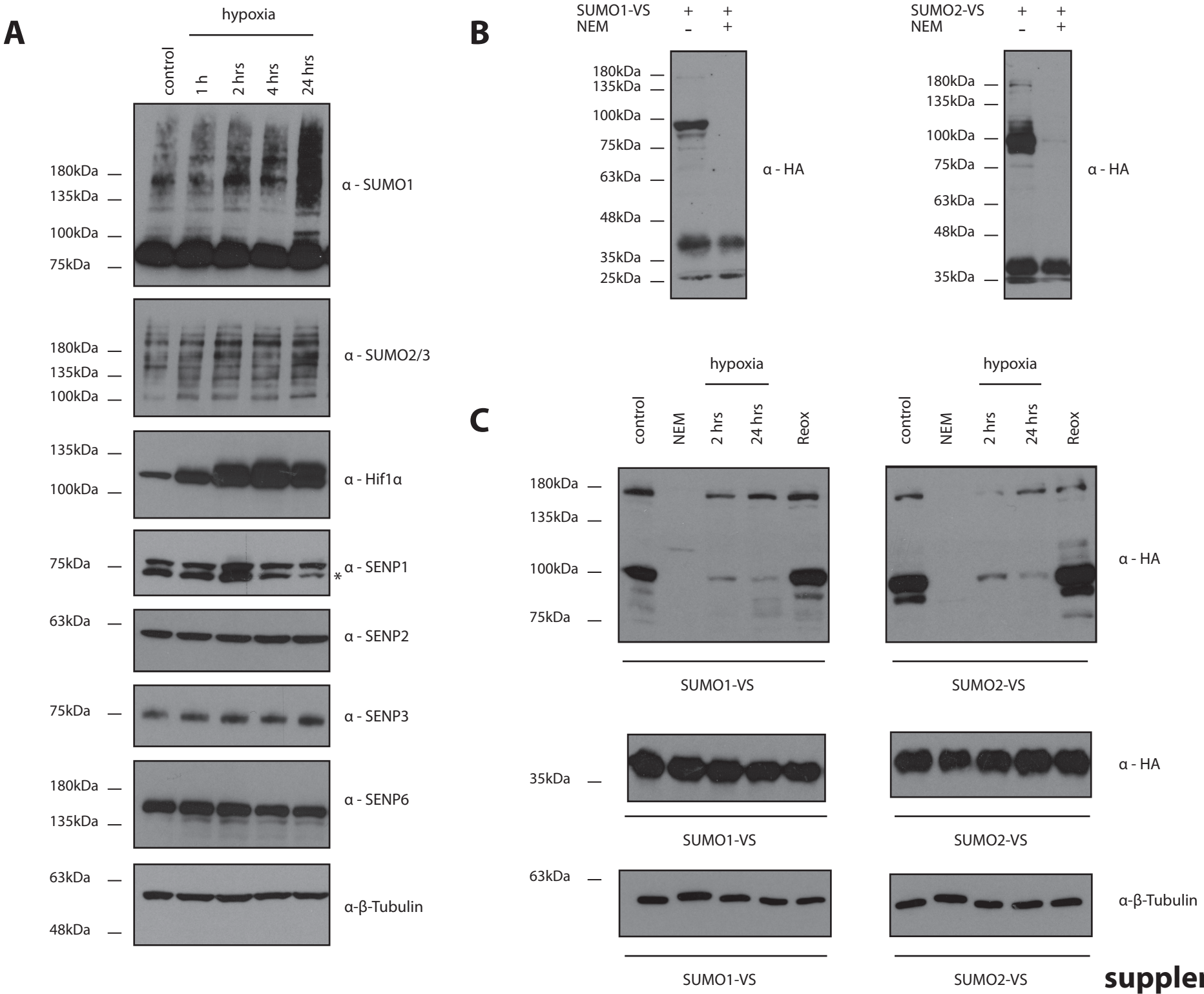

supplemental figure 2

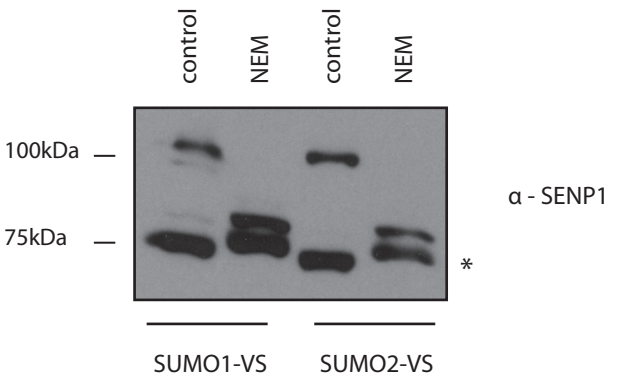

α - SENP1

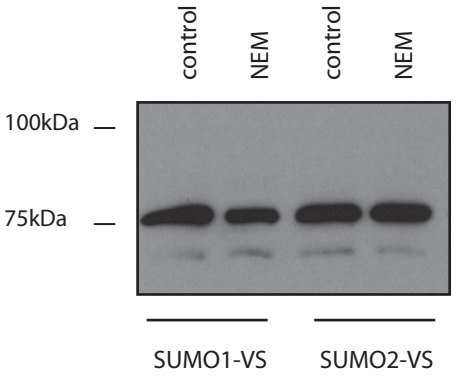

α - SENP2

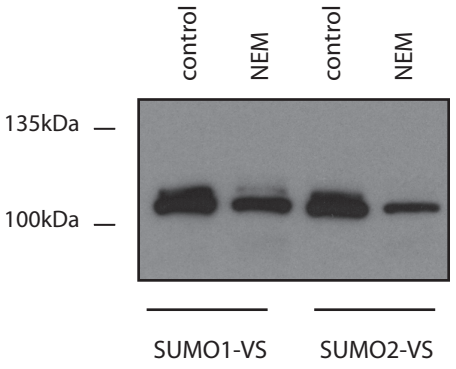

α - SENP5

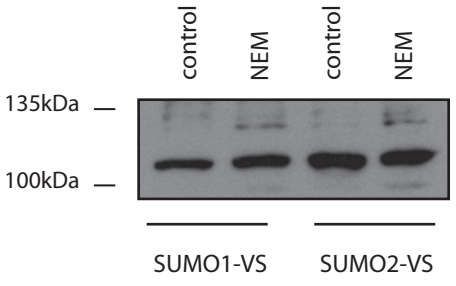

α - SENP7

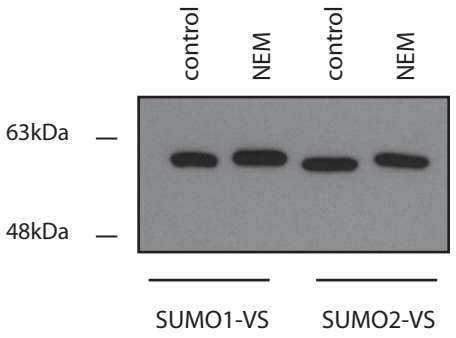

α-β-Tubulin

supplemental figure 3

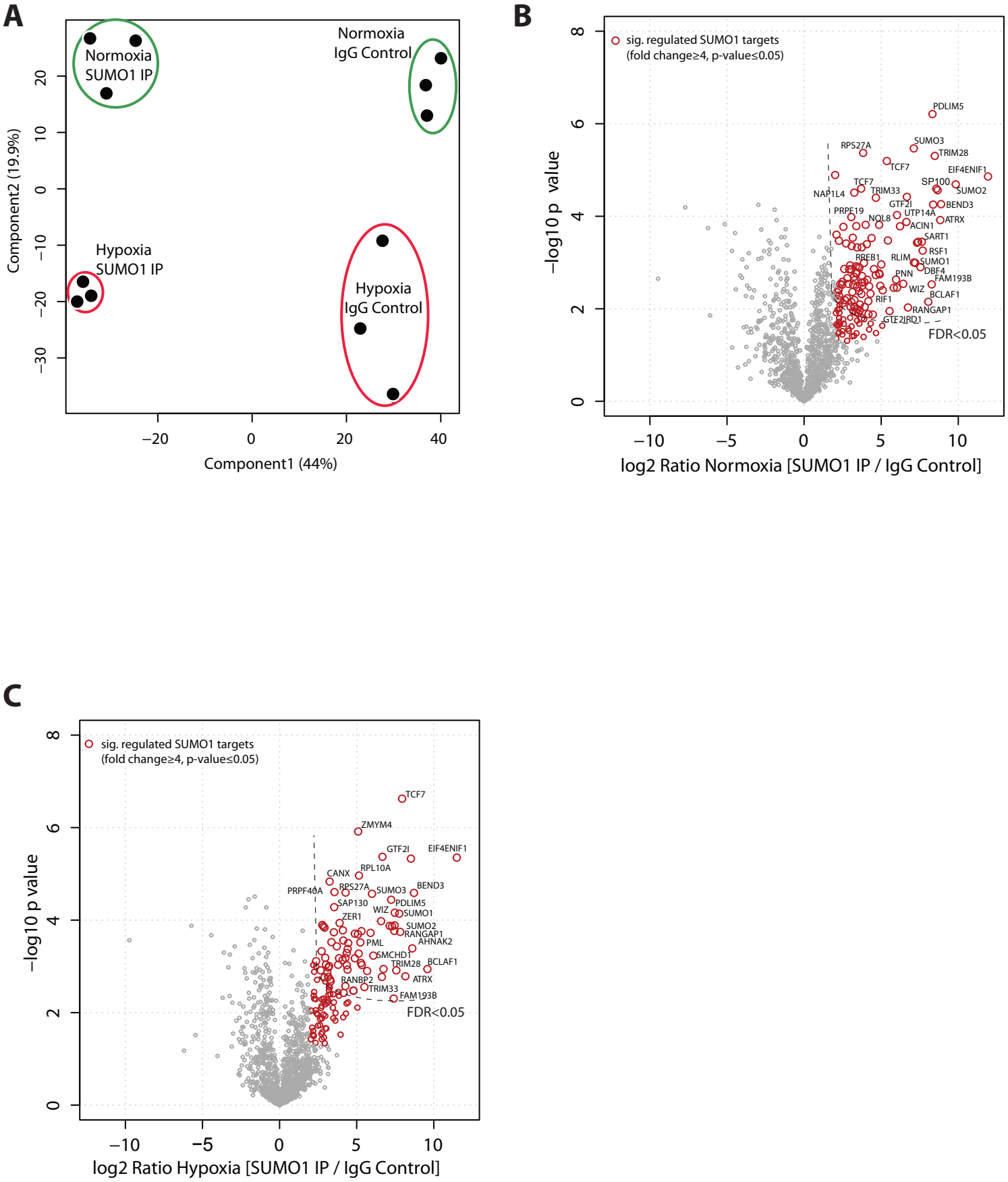

supplemental figure 4

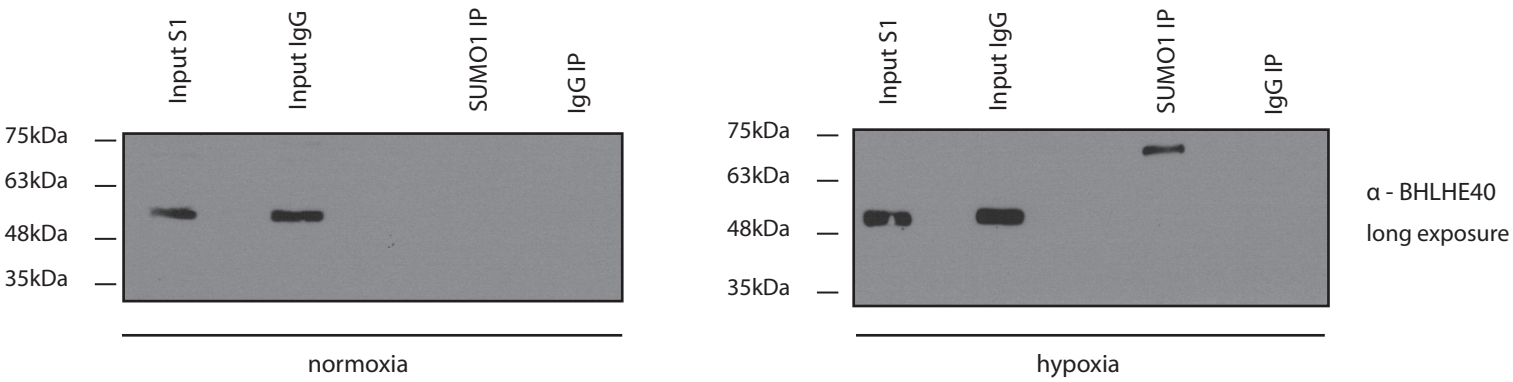

supplemental figure 5